Conf-910602--5

Analytical Simulation of Nonlinear Response to Seismic Test Excitations of HDR-VKL Piping System*

CONF-910602--5

DE91 006472

M. G. Srinivasan, C. A. Kot
Argonne National Laboratory, Argonne, IL 60439, USA
and
Masoud Mojtahed
Mechanical Engineering
Purdue University Calumet, Hammond, IN 46323, USA

To be submitted to:
The 1991 ASME PVP Conference
to be held in San Diego, California, June 23-27, 1991

* Work Sponsored by the U. S. Nuclear Regulatory Commission, Office of Nuclear Regulatory Research, under Contract W-31-109-Eng-38

Analytical Simulation of Nonlinear Response to Seismic Test Excitations of HDR-VKL Piping System

M. G. Srinivasan, C. A. Kot
Argonne National Laboratory, Argonne, IL 60439, USA
and
Masoud Mojtahed
Mechanical Engineering
Purdue University Calumet, Hammond, IN 46323, USA

ABSTRACT

The paper describes the analytical modeling, calculations, and results of the posttest nonlinear simulation of high-level seismic testing of the VKL piping system at the HDR Test Facility in Germany. One of the objectives of the tests was to evaluate analytical methods for calculating the nonlinear response of realistic piping systems subjected to high-level seismic excitation that would induce significant plastic deformation. Two out of the six different pipe-support configurations, (ranging from a stiff system with struts and snubbers to a very flexible system with practically no seismic supports), subjected to simulated earthquakes, were tested at very high levels. The posttest nonlinear calculations cover the KWU configuration, a reasonably compliant system with only rigid struts. Responses for 800% safe-shutdown-earthquake loading were calculated using the NONPIPE code.

The responses calculated with NONPIPE were found generally to have the same time trends as the measurements but contained under-, over-, and correct estimates of peak values, almost in equal proportions. The only exceptions were the peak strut forces, which were underestimated as a group. The scatter in the peak value estimate of displacements and strut forces was smaller than that for the strains. The possible reasons for the differences and the effort on further analysis are discussed.

INTRODUCTION

Dynamic tests with simulated earthquake excitation (SHAM) were performed during April–May 1988 on the Versuchskreislauf (VKL) piping system at the Heissdampfreaktor (HDR) Test Facility in Kahl/Main, Federal Republic of Germany. The major objectives of these tests were to study the behavior of a full-scale in-plant piping system subjected to a range of seismic excitation levels (from design levels to those that might induce either failure of pipe supports or plasticity in the pipe runs) and to establish seismic margins for piping and pipe supports. Data obtained in the tests are also being used to validate analytical methods for piping response calculation. Detailed reports on the SHAM experiments are given elsewhere by Kot et al. (1990).

This paper describes an effort to evaluate the computer code NONPIPE (proprietary to Nutech Engineers) with data from one of the SHAM tests. NONPIPE is a nonlinear finite-element program capable of calculating the elastic-plastic response of piping systems subjected to seismic excitation. The special characteristic of this code is the simplified or approximate approach it uses for modeling the elastic plastic behavior which makes the calculations relatively less resource intensive than those of other nonlinear codes. The evaluation is based on a comparison of computational results of simulation of a SHAM test with corresponding test measurements.

DESCRIPTION OF TESTS

Figure 1 shows the VKL piping system. The pipe runs of the VKL, excluding the HDU vessel, extend about 10 m in the vertical direction, about 11.5 m in the x direction, and about 6 m in the z direction. The pipes are of stainless steel, ranging from 100 to 300 mm in diameter. The HDU vessel was fixed at its base, and a displacement restraint in the x and z directions was provided by a structural frame located about one-third of the height of the vessel from its top. The DF15 manifold was directly attached to the floor, as indicated schematically in Fig. 1. Six different seismic support configurations, designed by different participants in the SHAM experiments (Kot et al., 1990), were used during the dynamic tests. Figure 1 shows a configuration with struts only for seismic supports. This is designated as the KWU configuration for identification purpose only.

During the SHAM tests, the dynamic excitation along the x direction was applied to two different points of the piping with the H5 and H25 actuators, as shown in Fig. 1. The excitation time-histories represented an integral multiple of a hypothetical safe-shutdown earthquake (SSE) with a peak acceleration of 0.6 g. Although it was the intent to apply the same excitation at the two points, the recorded accelerations on the two actuators turned out to be somewhat different. The tests covered a range of excitation levels from 100 to 800% SSE, with the higher levels inducing plastic strains in the pipe. An excitation level of 800% SSE means that the amplitudes of the hypothetical SSE acceleration history were scaled up by a factor of eight, while the duration and the waveform of the history remained unchanged. This paper concerns a test of the highest level of excitation, viz., 800% SSE, of the KWU configuration. The pipes were expected to suffer plastic deformations at this level of excitation.

About 300 channels of response were recorded during each test. The response quantities measured in the tests included pipe strains; accelerations on the pipe and the actuators; displacements on the pipes, actuators and pipe supports; and forces in the supports and the actuators. After the application of a two-stage low-pass filtering that eliminated frequency contents greater than 60 Hz, the data became available in the form of time histories.

ANALYTICAL SIMULATIONS

Both pretest predictions and posttest simulations of the linear response of the VKL system for different support configurations for low-level excitations have been performed in the past. Earlier reports (Kot et al., 1990, Srinivasan et al., 1989, Srinivasan et al., 1990) gave the results of the pretest and posttest linear simulations. These simulations were made with the piping subsystem module of the SMACS code (Johnson et al., 1981) which requires the input to be defined as acceleration histories and permits multiple independent history input. The responses calculated from the SMACS code generally were smaller than the corresponding test measurements. The finite element model devised for the

SMACS code simulations was used, with some changes, for the nonlinear simulation with the NONPIPE code. The major changes to the model for the NONPIPE calculations were the introduction of material properties in the plastic regime and the replacement of single curved pipe elements for elbows with multiple straight pipe elements.

Description of NONPIPE approach

The NONPIPE code, developed by and proprietary to Nutech Engineers (1984), is a finite-element program capable of determining the nonlinear dynamic response of piping systems of arbitrary configuration subjected to force or acceleration time histories. The nonlinearities modeled are elastic-plastic material behavior, gaps in connection to supports, and large displacement effects arising due to substantial change in direction of restraints. For the present problem the only nonlinearity considered was the elastic-plastic behavior.

Any number of input force histories, of arbitrary form, may be applied at any point of the piping system. However, the input acceleration is limited to a single set of three ground motion histories each of which is the acceleration along x, y, or z direction. The response calculated may be obtained in the form of time histories of pipe displacements, support forces, internal forces and moments at pipe sections, and kinematic quantities such as curvature or strains.

Elastic-plastic behavior is modeled by assuming the moment-curvature and torque-twist relationships to be trilinear. Strain hardening is approximated by considering the pipe element to consist of three parallel pipe elements, each with its own elastic-plastic or elastic behavior derived from the trilinear relationship. This is an extension of the approach used in the DRAIN-2D code (Kanaan and Powell, 1975). The yield criterion for each parallel element is assumed as follows:

$$\left[\frac{M_{xx}}{M_{pxx}}\right]^2 + \left[\frac{M_{yy}}{M_{pyy}}\right]^2 + \left[\frac{M_{zz}}{M_{pzz}}\right]^2 = 1$$

where M_{xx}, M_{yy}, and M_{zz} are computed bending moments and the torsional moment respectively. M_{pxx}, M_{pyy}, and M_{pzz} are the plastic bending moments and plastic torsional moment for the parallel element. The plastic moment (or torque) is defined as the maximum moment (or torque) the cross section can sustain if the material were elastic, perfectly plastic.

The system is assumed to have proportional damping. Consequently only two material parameters are needed to be input.

The Direct Stiffness method is used to perform the analysis in which the coupled equilibrium equations are solved for each step with a constant average acceleration assumption. The stiffness is modified each time a change in the yield status of the structure occurs, and correction forces are applied at the end of each time step to ensure that the dynamic equilibrium is continually satisfied.

Finite-Element Model

The entire system shown in Fig. 1 was modeled with pipe and spring elements only. The HDU vessel, the DF15 and DF16 manifolds, the spherical tee, and the valves were all approximated with pipe elements. The connection of the HDU vessel to the nozzles at its top was represented by artificial pipe elements of equivalent stiffness and zero mass density. Concentrated masses were added to the appropriate nodes to represent the actual mass of the parts represented by such artificial elements. A similar technique was used for modeling the tees and the valves. Each pipe elbow was modeled by means of five straight elements. The model comprised 266 pipe elements. The total mass of the system as modeled, including the concentrated masses, was about 78,400 Kg.

The preliminary results from the first attempt of simulating the test with NONPIPE showed that the deformations in the pipe at the point of attachment to the actuator at H5 were much higher than those measured. This was partly ascribed to the fact that the model neglected to take into account the additional stiffening of this region due to the actuator clamp. Subsequently the stiffness in this neighborhood was increased to correspond to the dimensions of the actuator clamp.

The pipe supports were modeled with spring elements. The constant-force hangers H16, H17, H18, and H19 were ignored since they were assumed not to respond to dynamic excitation. Although appropriate stiffness was assumed to represent each of the remaining pipe supports, no distinction was made as to the behavior of struts and spring hangers when subjected to dynamic excitation. The two sway struts of H23 were represented by a single spring element, implying the assumption that the forces in the two struts were always identical.

The spring elements were assumed to be hinged at their wall end and attached directly to the pipe nodes at the other end. Displacement and rotation restraints were specified at the appropriate nodes of the elements representing the HDU vessel and the DF15 manifold.

Inputs to Analysis

As noted before, the NONPIPE code does not provide for specifying multiple independent acceleration input. However, it does allow independent force histories to be prescribed. Both the acceleration and the displacement histories applied at each of the two actuators, H5 and H25, showed that the two inputs were not the same. Therefore it was necessary to apply the excitation in the form of equivalent force histories at H5 and H25.

The equivalent force may be determined in two ways. An artificial point mass (with a value many times larger than the total system mass) at the excitation point may be introduced and a force, obtained as a product of the applied acceleration and the introduced mass, is applied to this point mass. Alternatively, an artificial boundary spring element (with a stiffness that is many times larger than the largest stiffness in the system) may be introduced at the excitation point and a force, obtained as a product of the measured displacement and the stiffness of the introduced spring, is applied to the introduced spring element at its wall end.

In the first attempt of analysis with NONPIPE the former method was used to specify the input excitations. Instead of the measured accelerations at H5 and H25, acceleration histories derived as the second derivative of the measured displacement histories were used. The reasons and method for deriving these is described in a previous paper (Srinivasan et. al, 1990). As noted before, the preliminary results from this analysis showed that the calculated deformations in the neighborhood of H5 were very high compared to the test measurements.

One of the possible causes for this was suspected to be the high frequency peaks in the input accelerations which arose from the differentiation process. Consequently, it was decided to use the measured displacements for defining the excitation force and the latter method noted in the previous paragraph was used. The results reported in the paper actually correspond to the displacement excitation input.

Two spring elements were introduced, one each at H5 and H25. The stiffness of each of these elements was defined to be about a million times larger than that of the stiffest spring element. The excitation displacement histories were scaled up by the stiffness and defined as forces at H5 and H25.

Figures 2 and 3 show the measured displacements at H5 and H25 respectively. As may be noted from these figures the excitation actually begins at about 0.7 s after the clock is turned on and that the peak values for the histories occur before 5 s. Therefore the responses were determined only for the time between 0.7 s to 5.5 s. The digitization interval for the excitation histories was 0.0048624 s. The increment between analysis time steps was a fourth of the above, i.e. 0.0012156 s. Before the final computation, a parameter study was performed to ensure that the time step chosen did not give rise to significant error. In the parameter study solutions were determined for up to about 3 s (approximately 0.8 s beyond the onset of initial yielding) using two other time steps besides the above value. The other two time step values were 0.0000972 s and 0.0000486 s, corresponding to a fiftieth and hundredth of the digitization interval respectively. It was found that the differences in peak displacements and support forces for the different time steps were of the order of a fraction of a percent.

Strain hardening properties were specified for all the pipe elements except those that modeled such components as valves. These properties were derived from experimental stress-strain curves in uniaxial tension. Almost all the pipe runs were made of either of the two steels, denoted as DIN 1.4550 (10 Cr Ni Nb 18 9) and DIN 1.4961 (8 Cr Ni Nb 16 13). The stress-strain curve for these materials do not have a classical or well-defined initial yield stress and show nonlinear strain hardening. However, for the purpose of NONPIPE analysis, the stress corresponding to 0.2% offset strain was defined as the initial yield stress and the strain hardening part was approximated by a line. Table 1 gives these properties.

Table 1. Strain Hardening Properties of Pipe Materials

Material	Initial Yield Stress	Strain Hardening Modulus
DIN 1.4550	263.0 MPa (38145 psi)	3180 MPa (461.22 ksi)
DIN 1.4961	250.5 MPa (36332 psi)	4870 MPa (706.33 ksi)

NONPIPE computes the trilinear moment-curvature and torque-twist relationship for each pipe cross section, using the section and material properties and making some approximation assumptions (Nutech Engineers, 1984).

The two parameters to describe damping, α and β, were selected such that for the frequency range of 3 to 11 Hz, the damping was in the range of 2 to 3%. For frequencies below 3 Hz the damping increased with decreasing frequency and for frequencies above 10 Hz the damping increased with increasing frequency. Because the frequency content of the excitation was mostly within the frequency range noted above, the higher damping outside this range is not of concern. However the artificially high value of damping at higher frequencies was consistent with the recommendation to use higher damping at higher modes for the sake of numerical stability. Anchoring the modal damping to be 3% at 2.5 Hz and 11 Hz, α and β were determined to have values of 0.748 and 7.22×10^{-4} respectively.

RESULTS OF CALCULATION COMPARED WITH MEASUREMENTS

Displacements corresponding to 16 measurement channels, forces in all the struts and variable-force hangers, and bending and shear strains at 11 measurement locations were computed. Only a few of these are presented here. Figure 4 shows the locations for which comparisons of calculated and measured responses are given.

Figures 5-7 show the comparison of displacement components at gage location QN101. At this location the z component is better estimated than the other two components. The x measurement , however, is suspect because the oscillations are very much skewed towards the positive direction. Much better comparison for the x component is obtained at location QN122 as seen in Figure 8. In general, when all the comparisons are considered, the z components were overestimated by 15 to 35 %. About half of the y components were underestimated while the other half were overestimated. Two out of the three x components computed were close to the measurements.

Figures 9 and 10 show the comparison of axial forces in struts H9 and H10. The peak force in H9 is overestimated and that in H10 is only very slightly underestimated. In fact the waveform for the force in H10 is very closely predicted. The force in H11, not shown, is also only slightly underestimated and the wave form is closely estimated. The peak forces in H4 and H23 are underestimated by 14%, and 60% respectively. In general, the strut forces are underestimated to various degrees, with H9 being the only exception.

Figures 11-14 show the bending strains at two straight pipe sections, RA760 and RA 763. These two locations are among the highly strained straight pipe sections at which measurements were made. At each section, a bending strain is labeled as y or z strain, corresponding to whether the strain is at the extreme fiber intersecting the local y or z axis respectively. The local x axis coincides with the pipe axis. At RA760, the calculated y-bending strain closely matches the measurement. However, the z-bending strain at this location does not match well, with the calculation overestimating the strain. At location RA763, the calculated y-bending strain is close to the measurement only up to about 4.2 s after which it deviates from the measurement. The calculated z-bending strain also deviates significantly from the measurement after about 4.2 s. This location is somewhat of an outlier in that the bending strain at no other location deviates as much from the measurement as at this. The comparison of bending strains at many cross sections, including those at elbows, shows that for most sections the wave form of the calculated bending strains does resemble that of the measurements. At locations other than the two shown, about half of the peak values are overestimated by 23 to 113% and the other half are underestimated by 10 to 33%.

Figures 15 and 16 show the comparison of measurement and calculation for shear strains at RA760 and RA763. As in the case of bending strains at RA763, the calculated strains begin to significantly deviate from measurement after about

4.2 s. For times smaller than 4.2 s, the calculation and measurement show similar trends and amplitudes though the waveforms do not match closely. Almost all the straight pipe sections and an elbow section for which comparisons were made show the same characteristics. The peak values at all other straight pipe sections is overestimated by 28 to 381% mainly because of this deviation after 4.2 s. At the elbow sections, the calculations underestimate the peaks at three locations by 10,42 and 45%, and overestimate the peak at two locations by 15 and 99%.

Discussion and Conclusion

Visual comparison of all the calculated histories with their measured counterparts showed that, qualitatively, the calculation results were hard to characterize as generally overestimates or underestimates. For some locations the time trend and amplitude were close to the measurement, for others they were different. A somewhat similar trend was observed in the SMACS calculations also. To provide a quantitative comparison and to obtain explanations for the differences between calculations and measurements, the peak value of each history was selected as representative of that history. The ratio of each calculated peak value to its measured counterpart was determined. The sample mean and the standard deviation, σ, for each type of response were computed and the results are shown in Table 2.

Table 2. Ratio of calculated peak value to measured peak value.

Displacement		Strut Force		Bending Strain		Shear Strain	
Mean	σ	Mean	σ	Mean	σ	Mean	σ
1.004	0.310	0.8422	0.276	1.2333	0.603	2.8945	4.025

A mean value smaller than unity indicates underestimation, and Table 2 shows that only the strut forces were underestimated as a category. However, the statistics shown in Table 2 could be misleading if it is not considered together with the comparison of the histories. As noted above, for the most part the calculations do give waveforms similar to those measured except in the case of strains for which large discrepancies occur for later times.

The relatively large value for σ in Table 2 for displacement and strut force shows that the scatter in the peak values is significant. Similar scatter was also observed in the results of the linear analysis although in the case of the present calculations the calculations generally give better qualitative, i.e. waveform, results. It has not been possible to trace the discrepancies to any specific modeling error or any error in the test data.

A possible source of error in the estimated strut forces, is the neglecting of gaps in the connections of supports to pipes. Examination of the test responses shown in Figs. 9 and 10 reveals that there were higher frequency oscillations in the measurements that the calculations fail to produce. Impacts that occurred as the gaps closed might be responsible for these higher frequency oscillations.

There are two probable reasons for the large discrepancies in some of the strain estimates. The first is the approximations involved in calculating the trilinear moment-curvature (and torque-twist) relationships although this is not expected to be very significant. The second and more significant factor concerns the large deviations for times beyond 4.2 s.

The elastic-plastic properties used for the materials and given in Table 1 were obtained from test specimens that did not come from the actual pipe runs of the VKL system. They are most probably from similar pipes that have never been loaded beyond initial yield. On the other hand, the actual pipes of the VKL had undergone a loading history that included repeated loading and unloading beyond the initial yield of the pipe. As a consequence of this, much of VKL piping had strain-hardened well beyond yield before the beginning of the test under consideration here, as documented by Schrammel et. al. (1988) for a location close to RA760. Consequently the analytical model was 'softer' than the actual pipe material. This seems to have caused the NONPIPE calculations to show significant ratcheting to occur at a time approximately about 4.2 s at many straight pipe sections. Since shear strains are better indicators of yielding than individual bending strains, many shear strain estimates show this as is illustrated clearly by Fig. 16.

Considering the nonlinear nature of the problem and the approximations involved in modeling inelastic behavior, the discrepancies in the NONPIPE-calculated response estimates are not unreasonably large. If information on the actual inelastic behavior of materials is available, NONPIPE might be an acceptable code for calculating an approximate estimate of plastic deformations.

In the present case, even though it is not possible to obtain the actual amount of strain hardening of the pipes, an effort is in progress to reduce the approximations involved in obtaining the moment-curvature relationships. This effort also includes the introduction of gaps in the support connections. It is expected that some improvements will be obtained in the response estimates calculated with NONPIPE due to these changes.

ACKNOWLEDGMENT

This work was performed under the sponsorship of the U. S. Nuclear Regulatory Commission, Office of Nuclear Regulatory Research. The authors wish to thank Dr. Akhil Gantayat of Nutech Engineers and author of the NONPIPE for his expert help during the model preparation and for the timely completion of the tasks for executing NONPIPE runs.

REFERENCES

Johnson, J. J., Goudreau, G. L., Bumpus, S. E., and Maslenikov, O. R., 1981, "Phase I Final Report— SMACS—Seismic Methodology Analysis Chain with Statistics (Project VIII)," NUREG/CR-2015, Vol. 9., Lawrence Livermore Laboratory.

Kanaan, A. E., and Powell, G. H., "DRAIN-2D , A general purpose computer program for dynamic analysis of inelastic plane structures, User's Guide and Supplement", 1975, Report No. EERC 73-6 and EERC 73-22, Earthquake Engineering Research Center, Berkeley, Ca.

Kot, C. A., Srinivasan, M. G., Hsieh, B. J., Malcher, L., Schrammel, D., Steinhilber, H., and Costello, J. F., 1990, "SHAM: High-Level Seismic Tests of Piping at the HDR," *Nuclear Engineering and Design*, V. 118, pp 305-318.

Nutech Engineers, Program NONPIPE Version 5.3 - User's Manual, 1984, NUTECH Engineers, San Jose, California.

Schrammel, D., Steinhilber, H., and Malcher, L., 1988, "Servohydraulische Anregung Maschinentechnik - Quick Look Report Versuchsgruppe SHAM

Versuch T41", (in German) PHDR Technical Report No. 86-88, Kernforschungszentrum Karlsruhe, page.29

Srinivasan, M. G., Kot, C. A., and Hsieh, B. J., 1989, "Response of HDR-VKL Piping System to Seismic Test Excitations - Comparison of Analytical Predictions and Test Measurements," *Trans. Tenth International Conference on Structural Mechanics in Reactor Technology*, Vol. K2, pp. 751-756.

Srinivasan, M. G., Kot, C. A., and Hsieh, B. J., 1990, "Analytical Simulation of Seismic Testing of VKL Piping System at the HDR Test Facility," *Seismic Engineering - 1990, The 1990 Pressure Vessels and Piping Conference, Nashville, Tennessee*, PVP-Vol. 197, ASME, New York, NY, pp. 175-182.

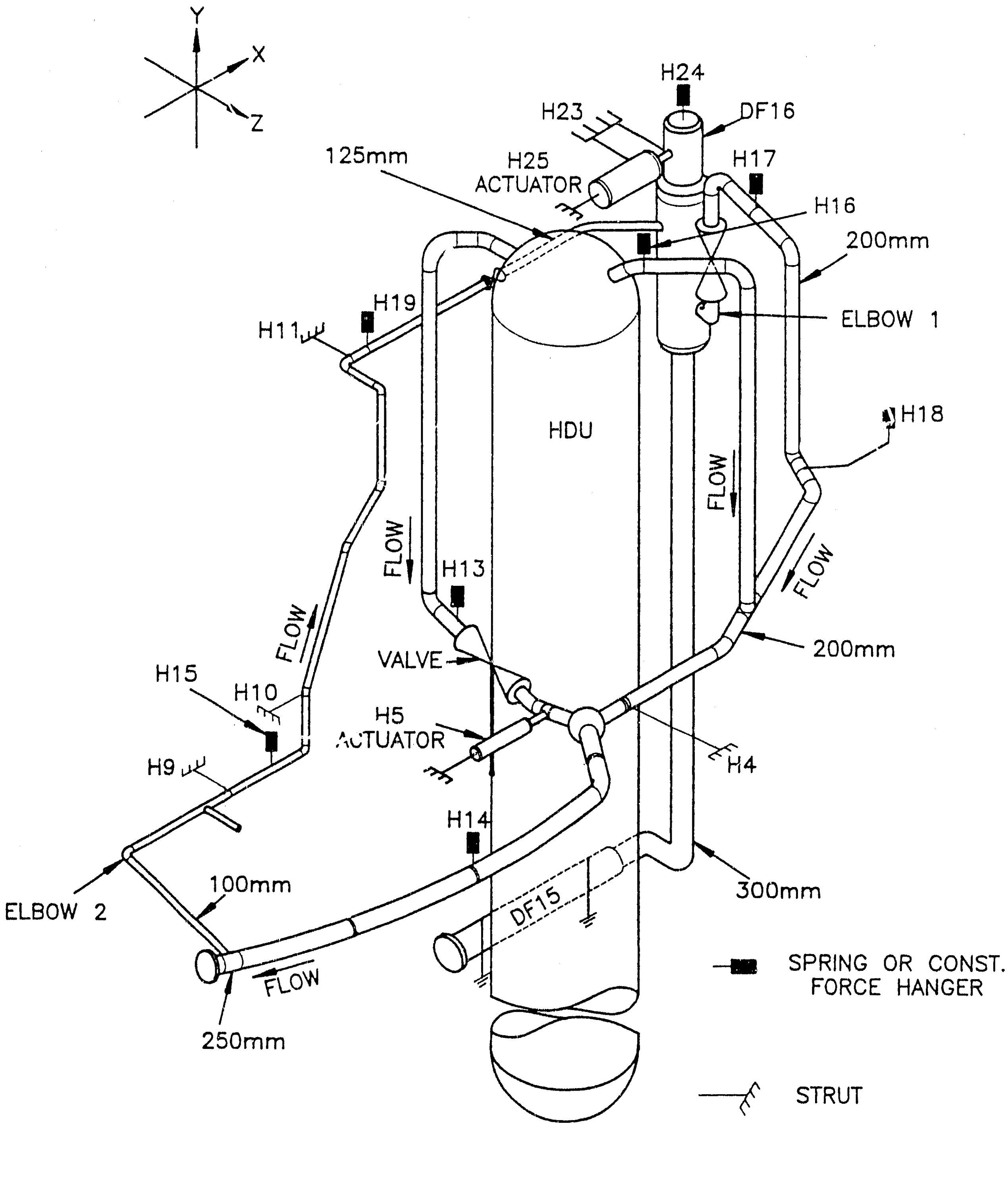

Figure 1. VKL Piping System with KWU Support Configuration

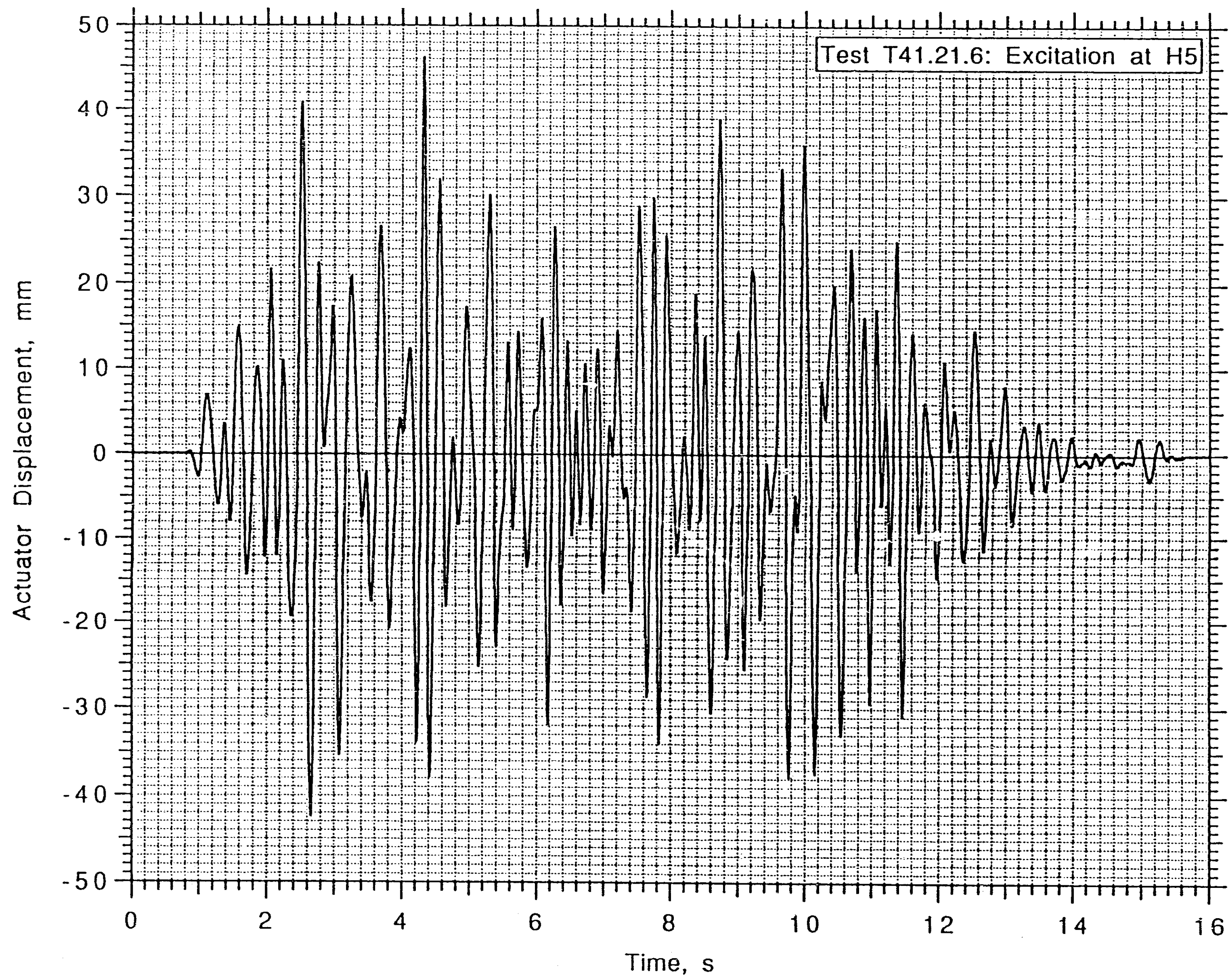

Figure 2. Measured Actuator Displacement at H5

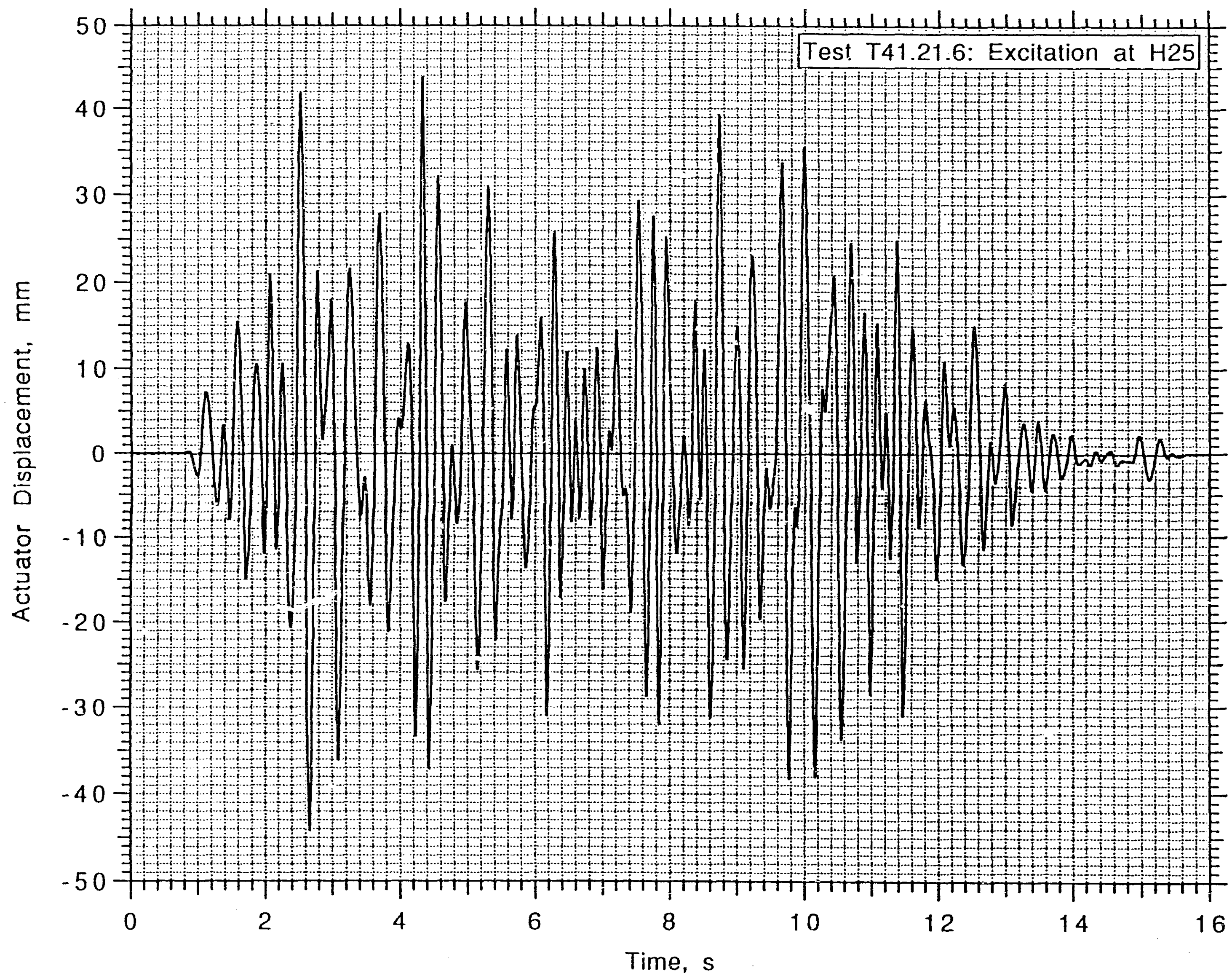

Figure 3. Measured Actuator Displacement at H25

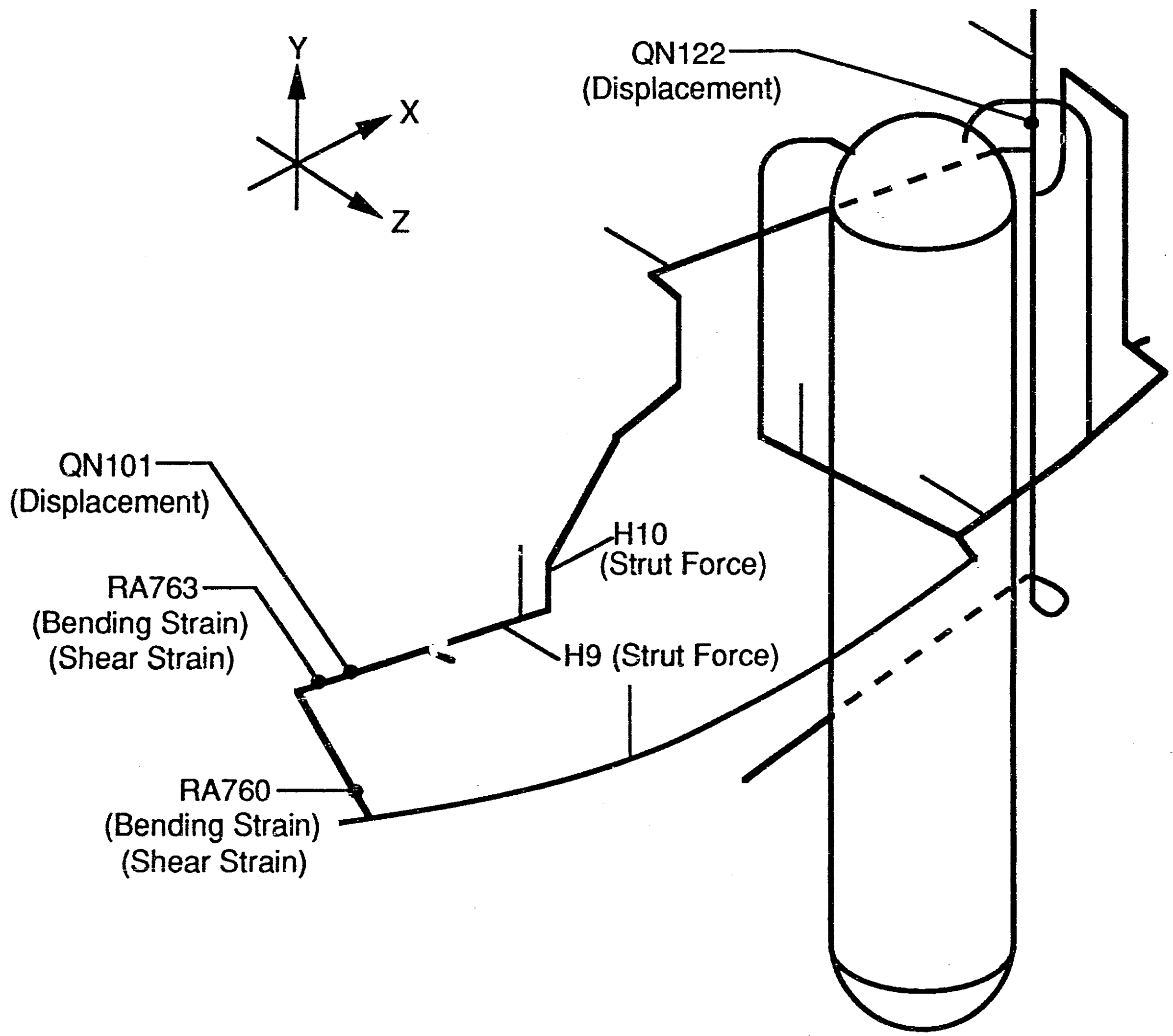

Figure 4. Locations for comparisons of response

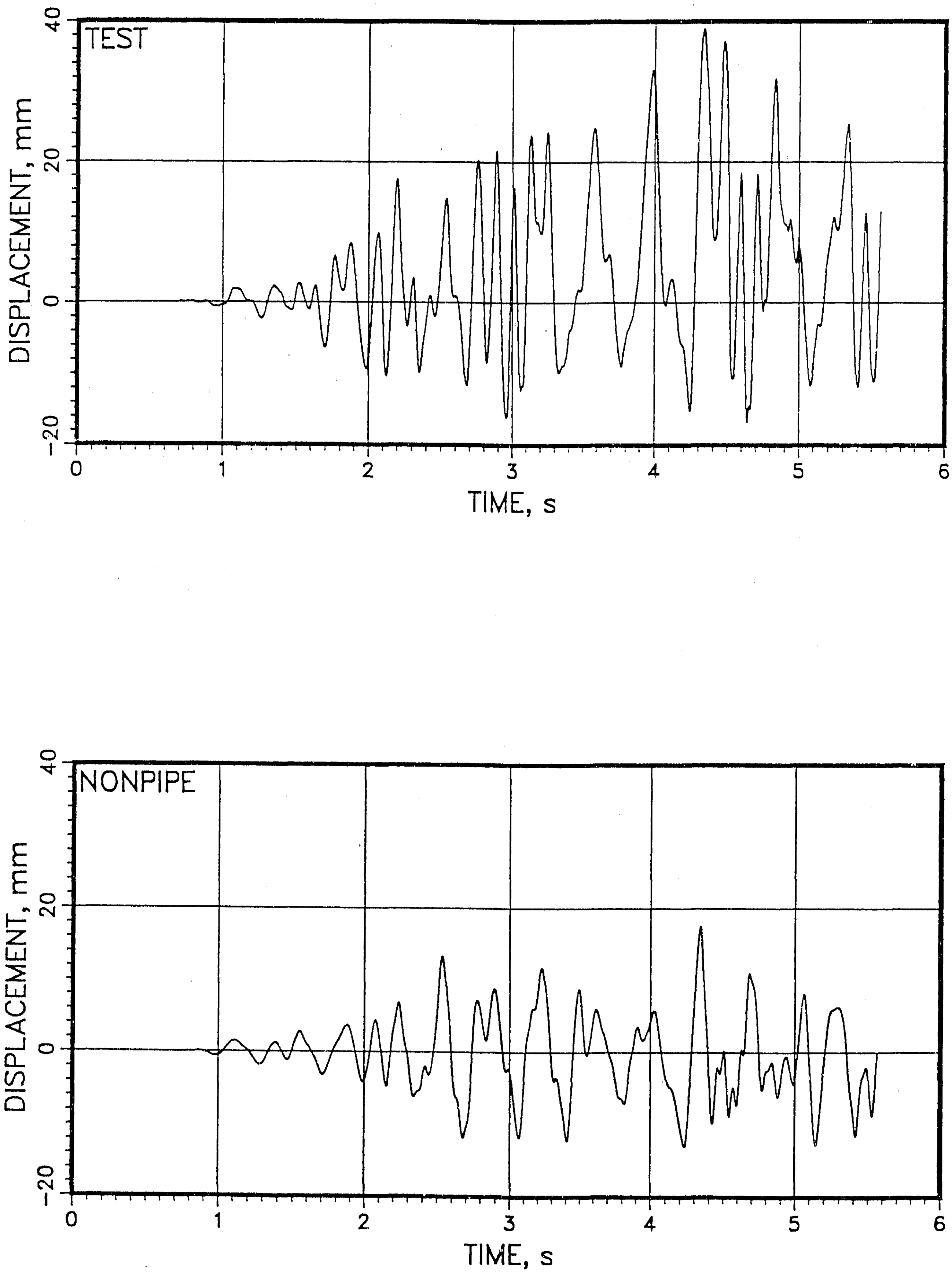

Figure 5. Comparison of measured and calculated x displacement at QN101

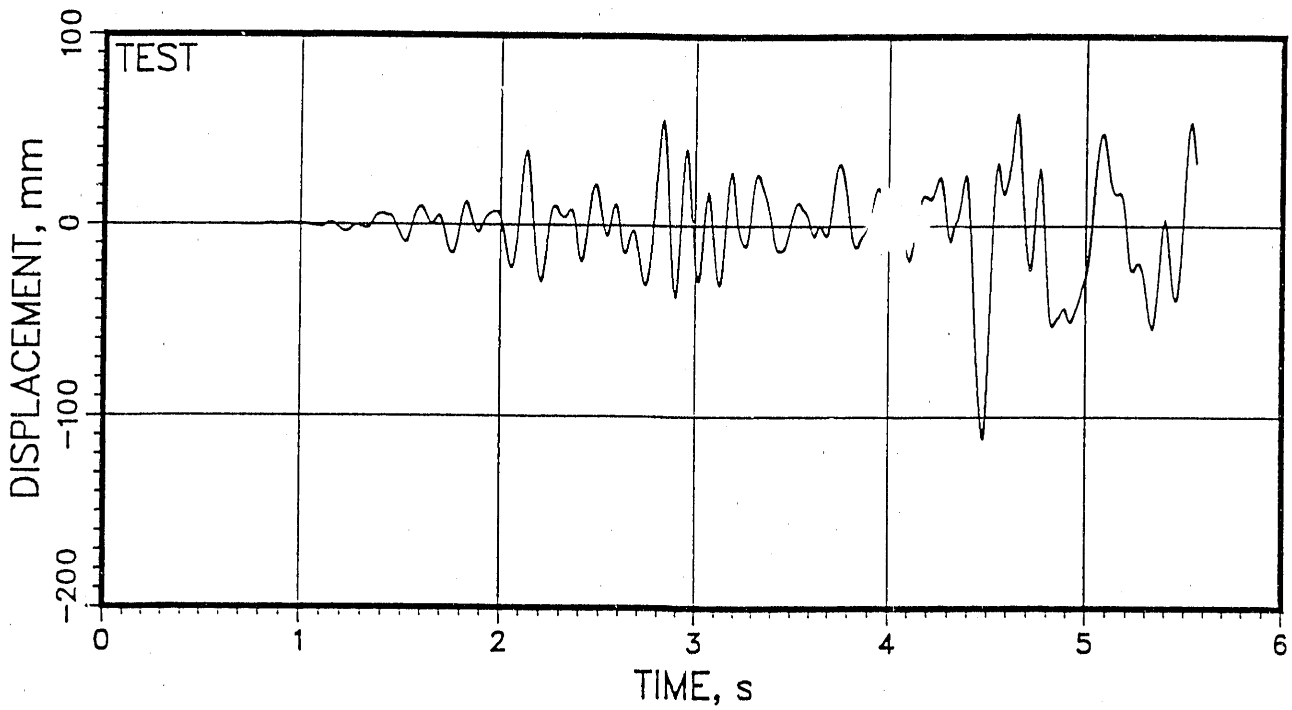

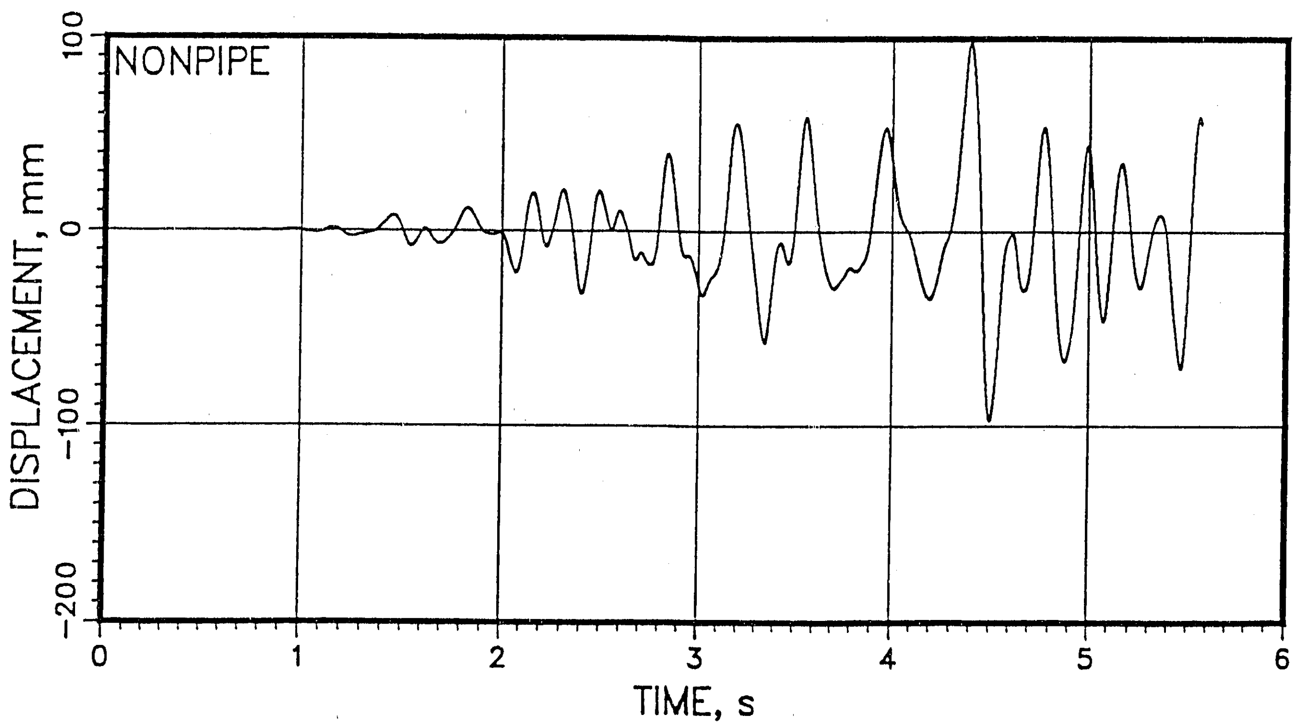

Figure 6. Comparison of measured and calculated y displacement at QN101

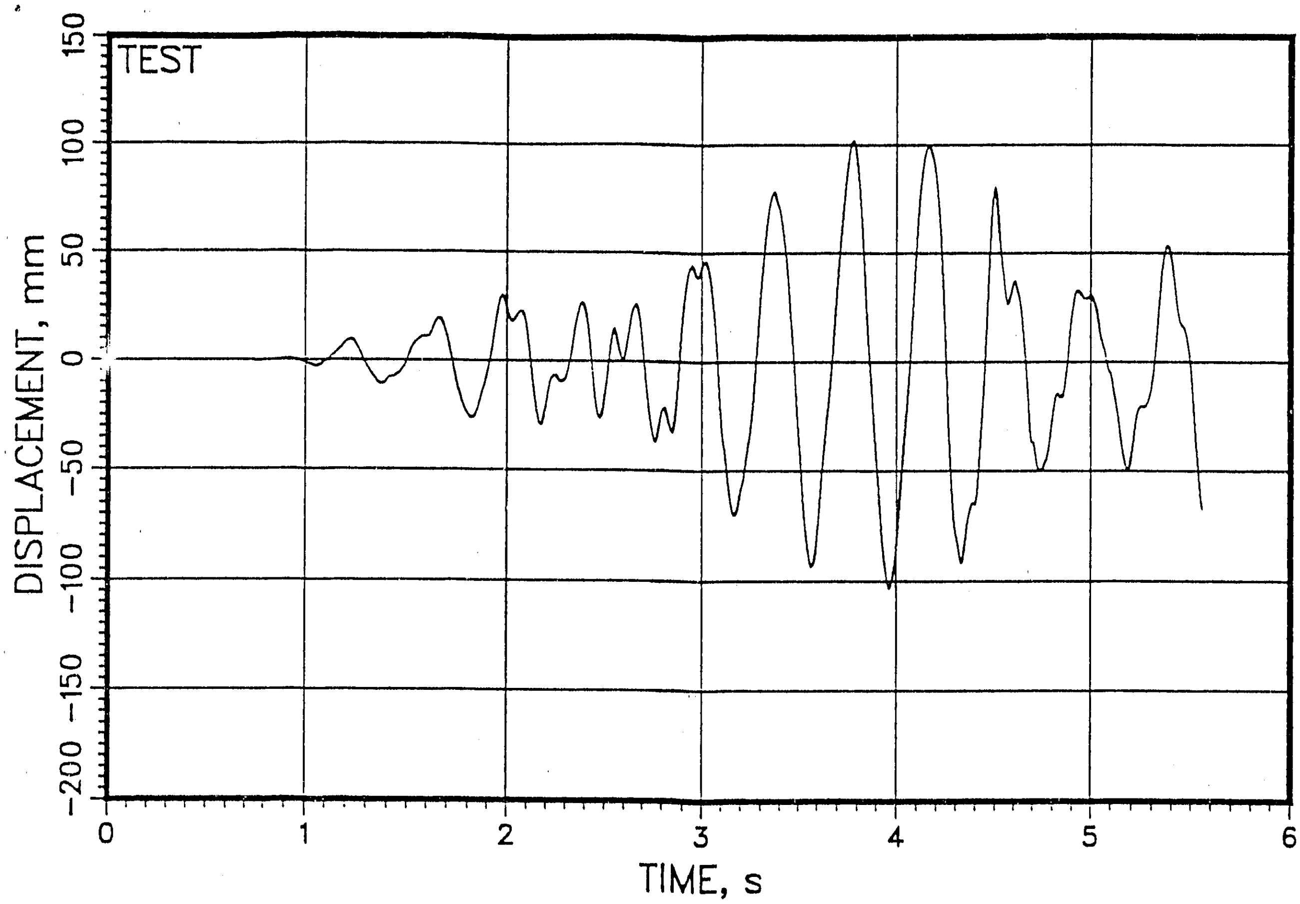

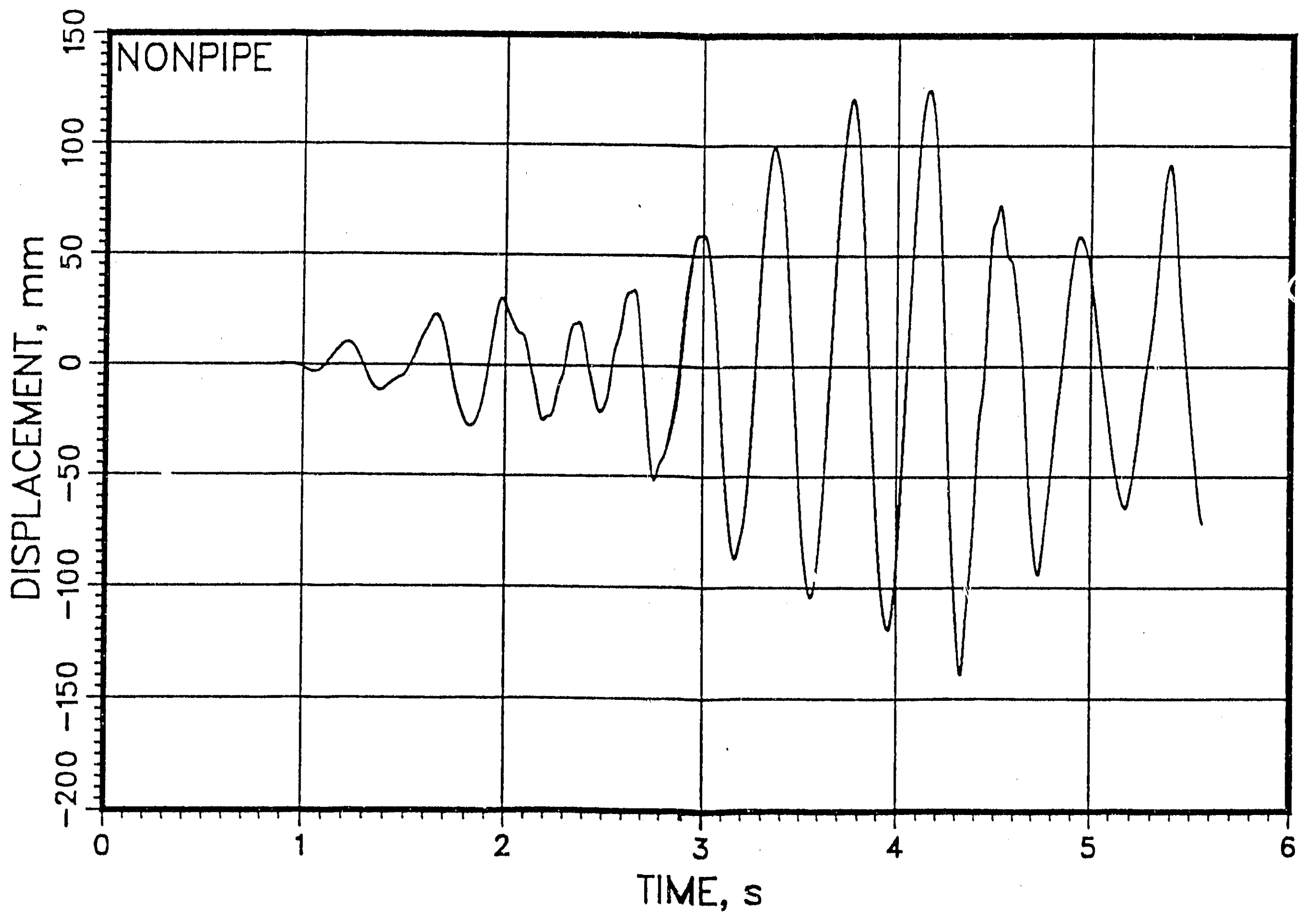

Figure 7. Comparison of measured and calculated z displacement at QN101

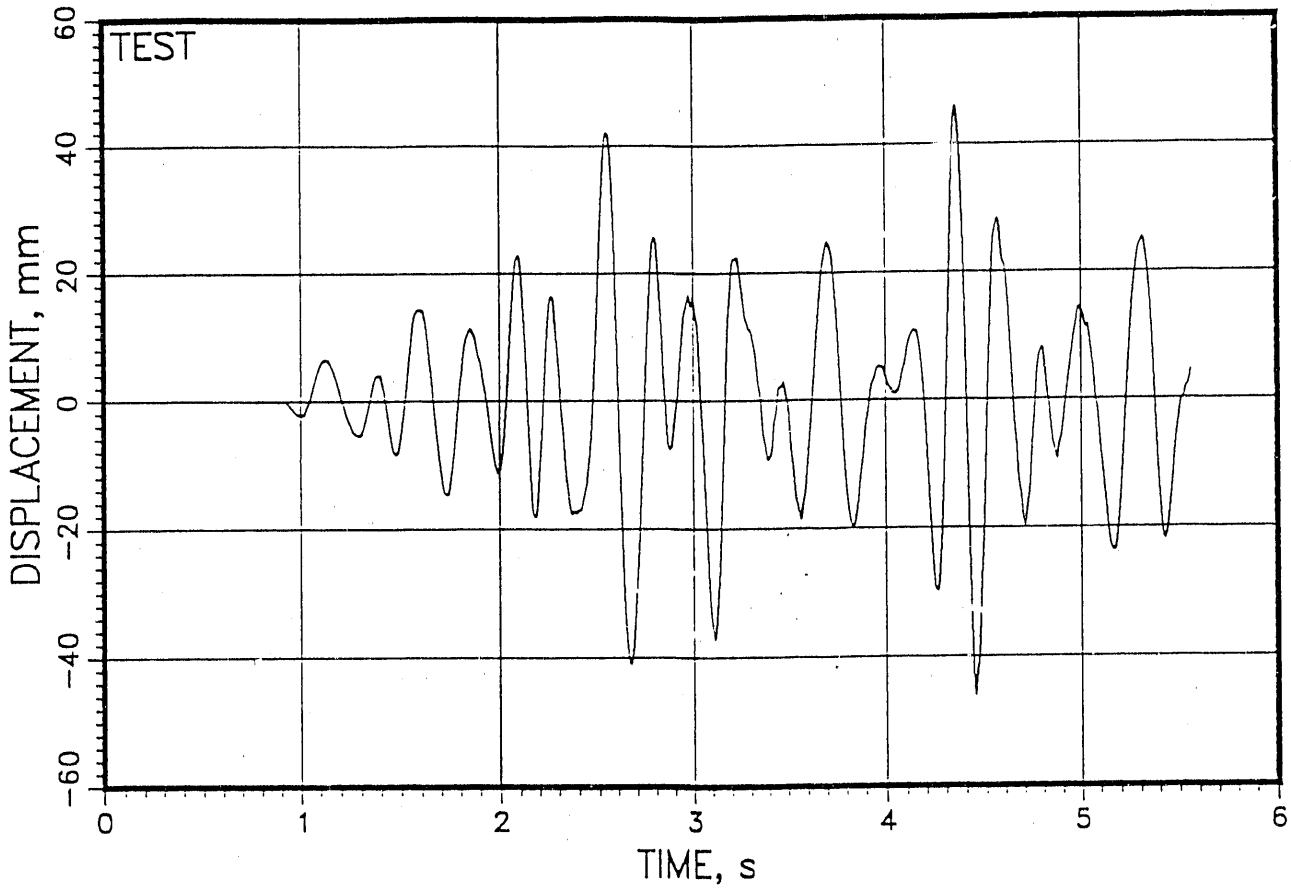

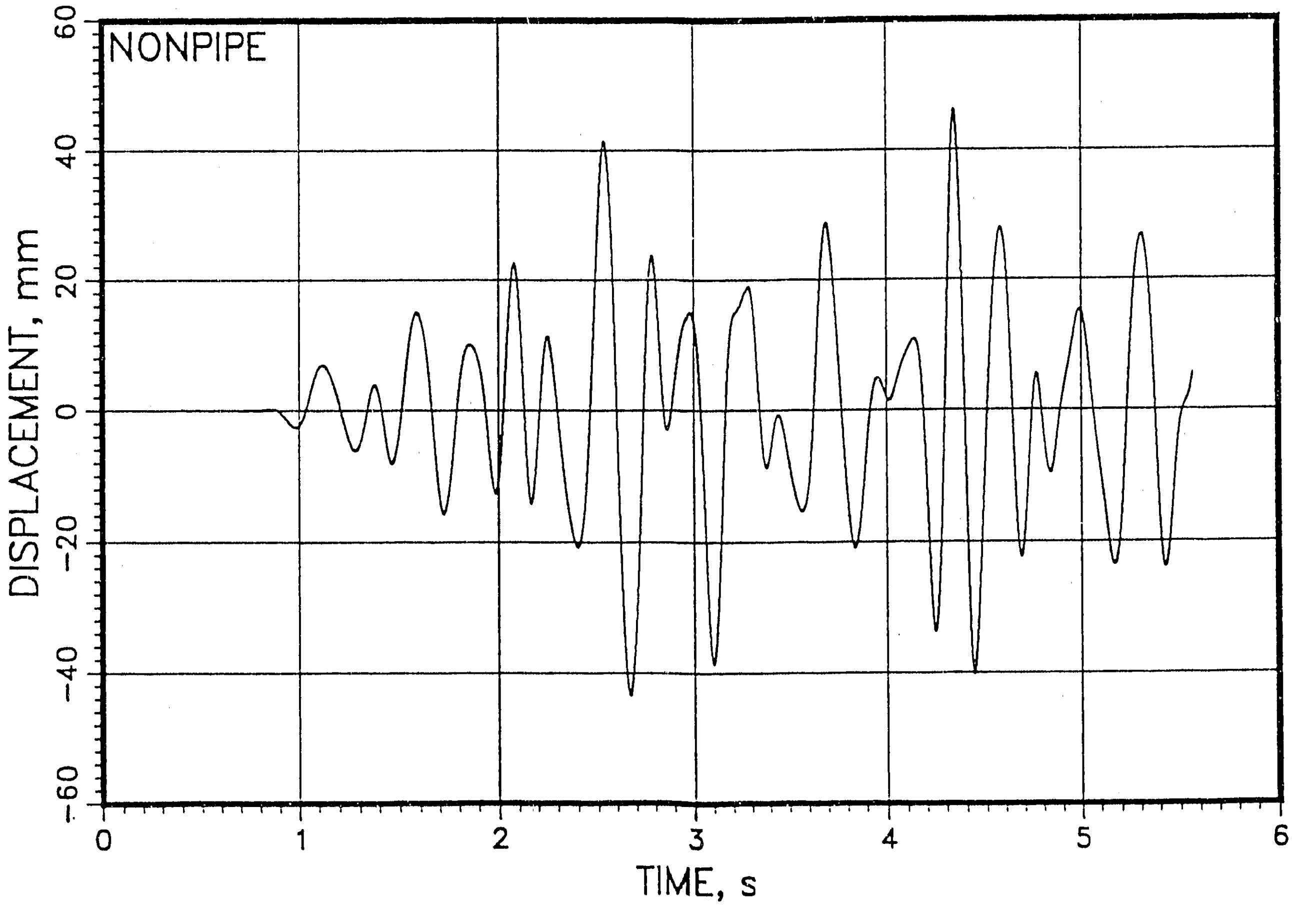

Figure 8. Comparison of measured and calculated x displacement at QN122

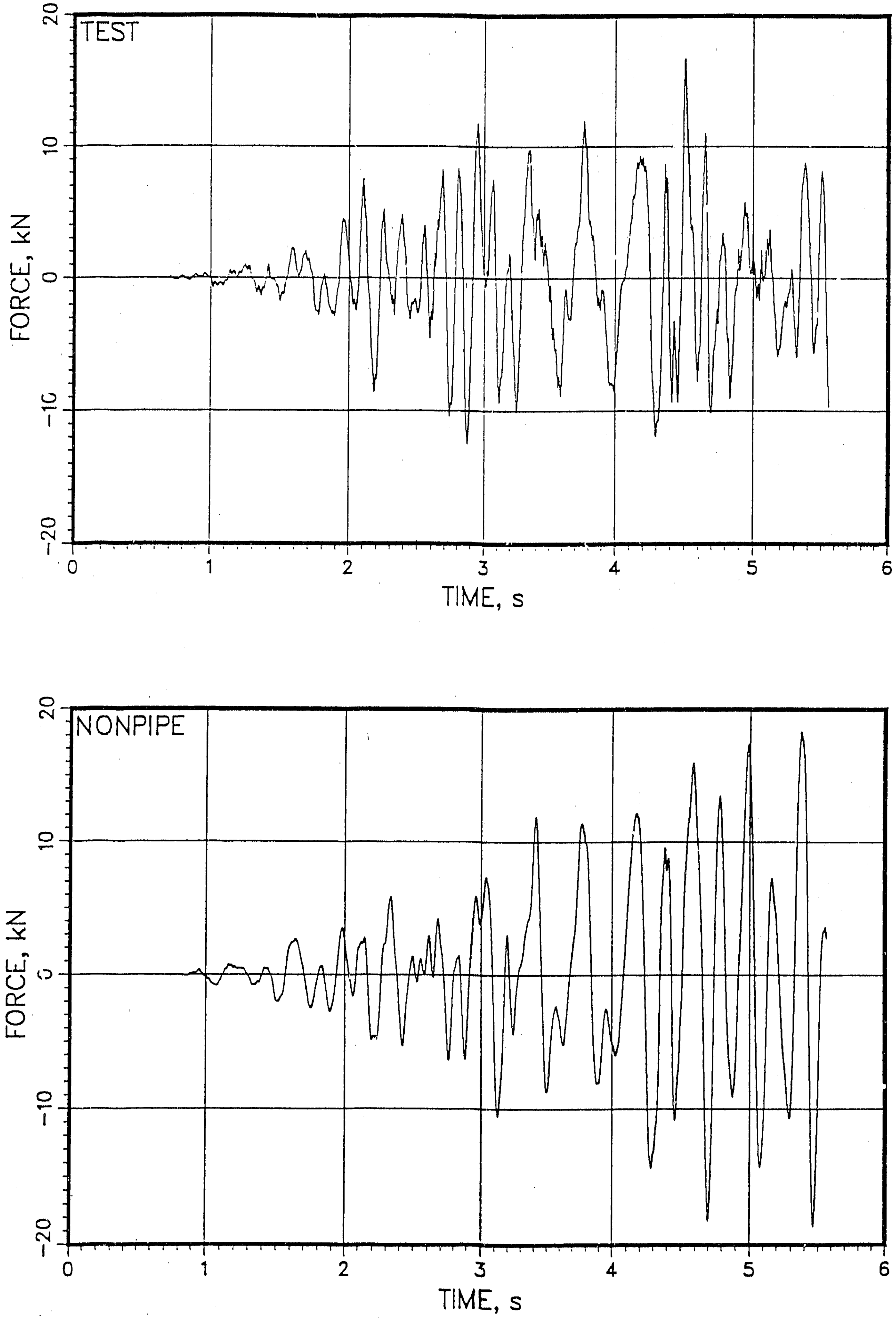

Figure 9. Comparison of measured and calculated force in strut H9

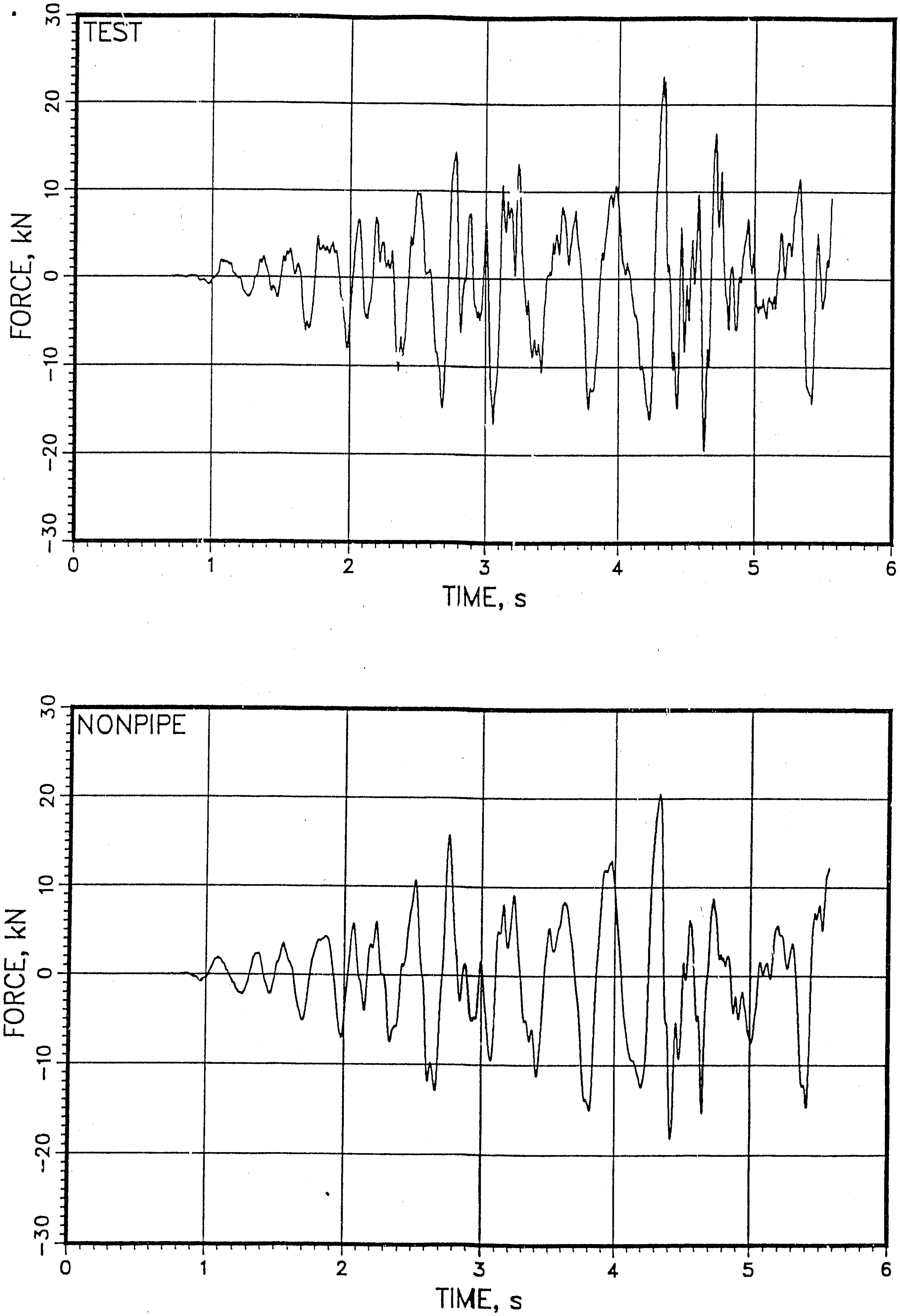

Figure 10. Comparison of measured and calculated force in strut H10

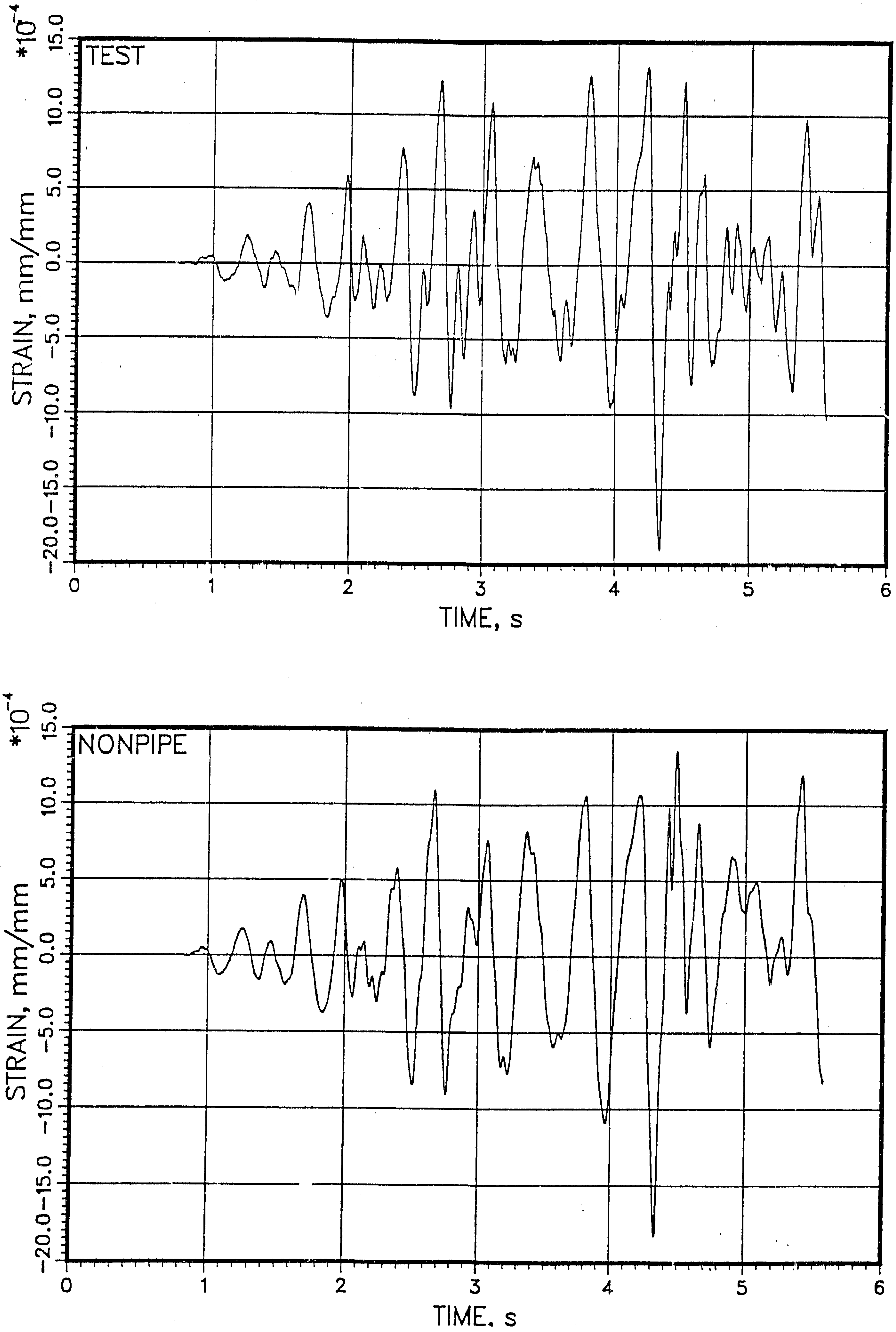

Figure 11. Comparison of measured and calculated y-bending strain at RA760

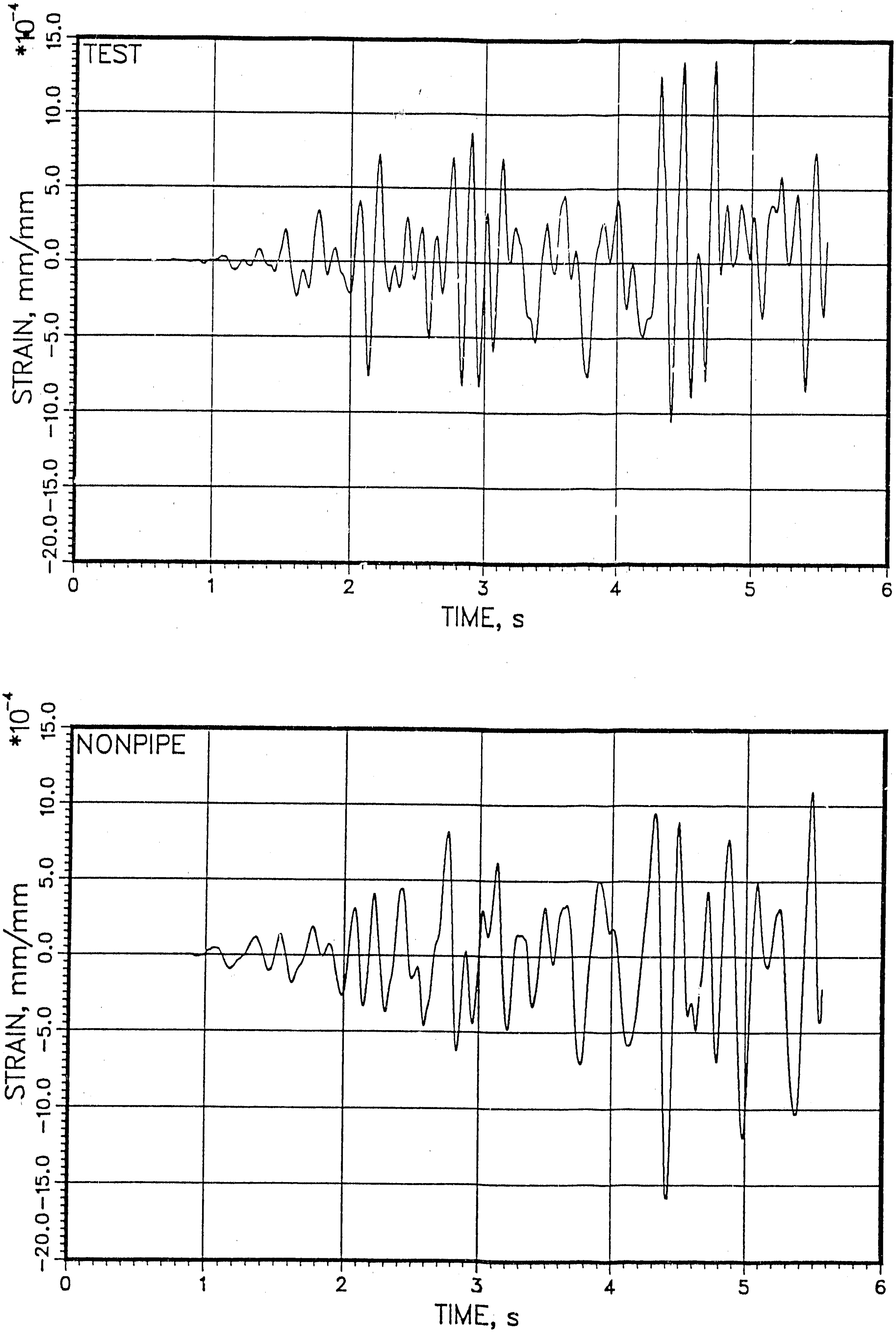

Figure 12. Comparison of measured and calculated z-bending strain at RA760

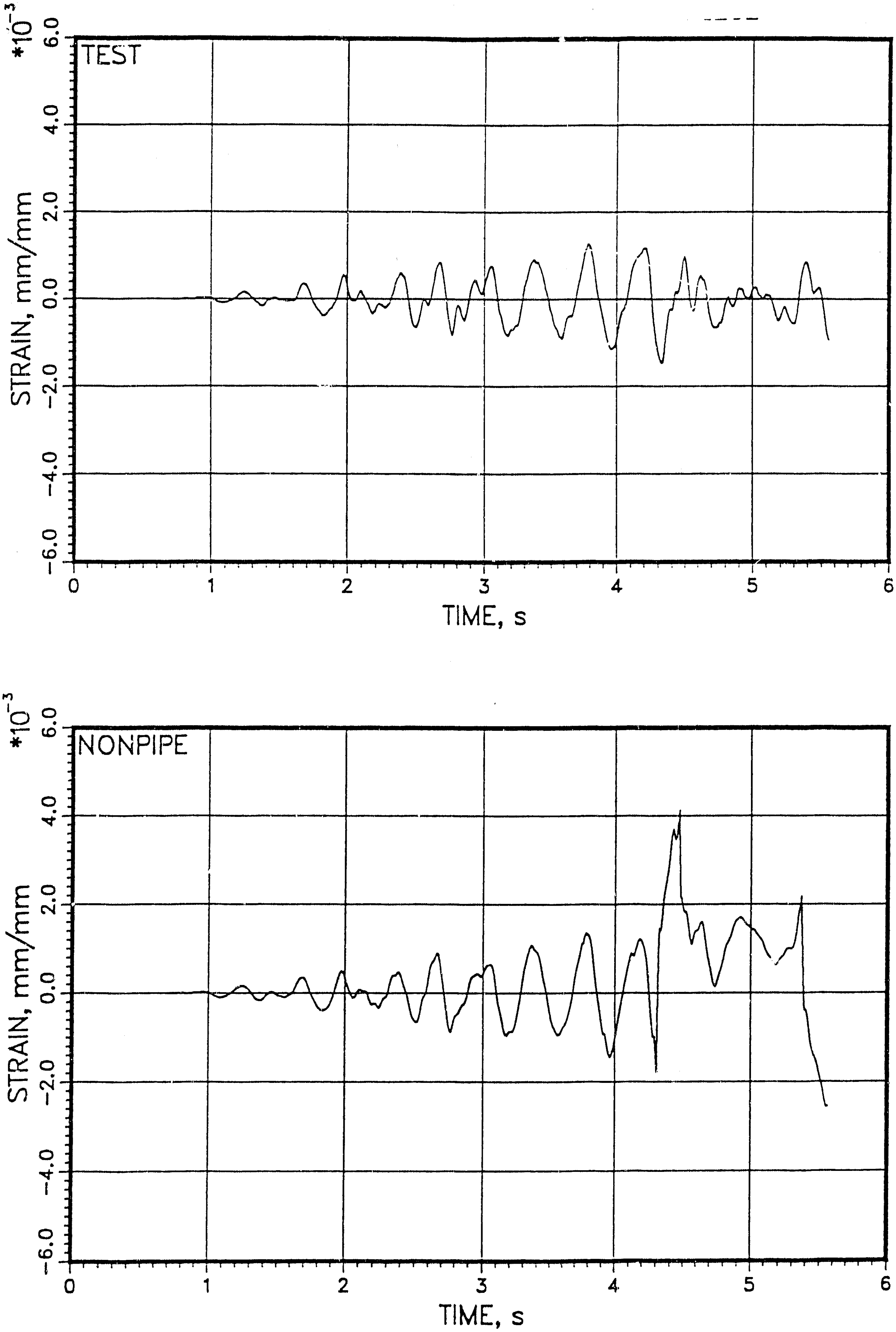

Figure 13. Comparison of measured and calculated y-bending strain at RA763

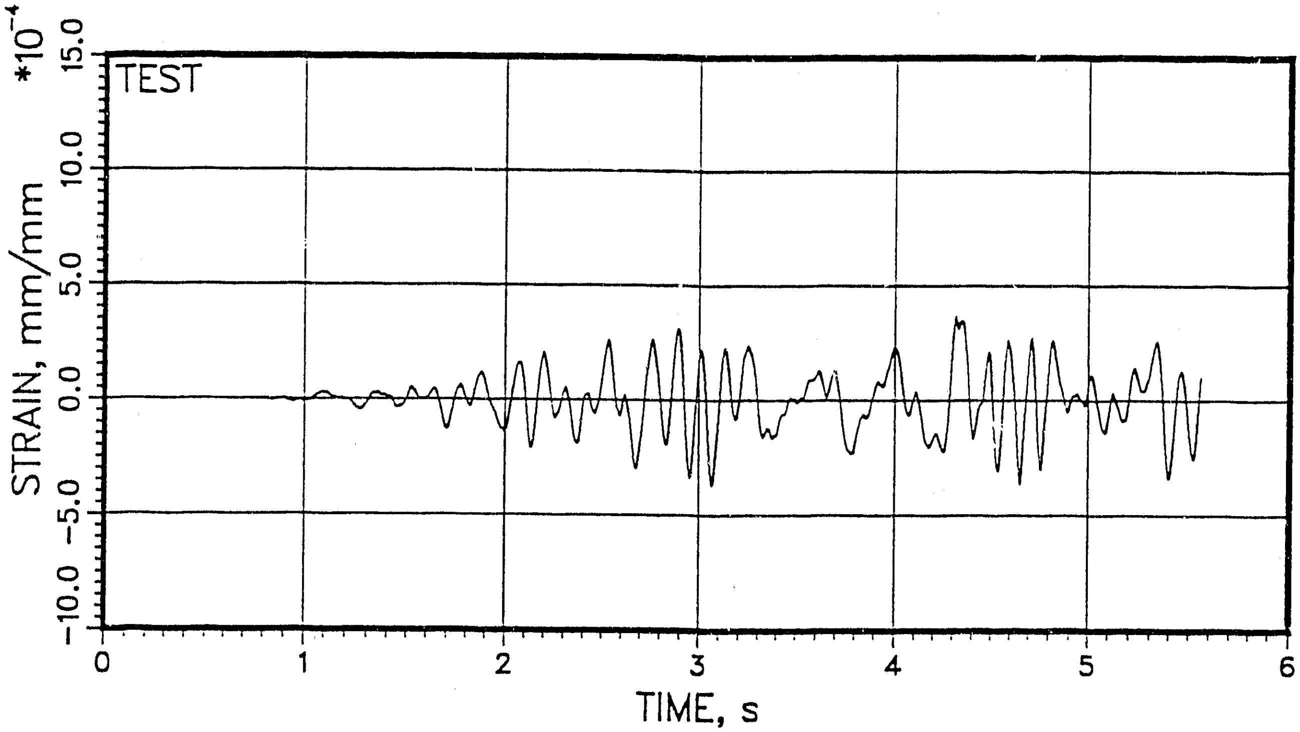

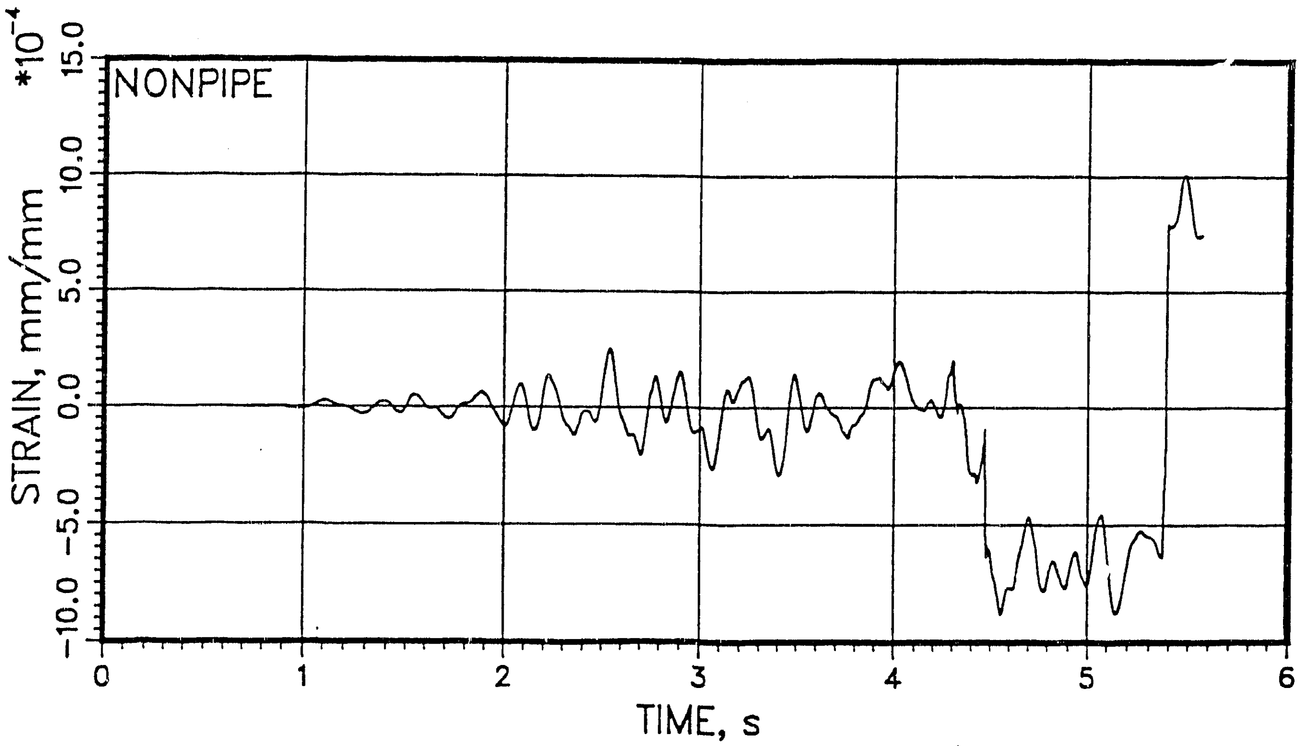

Figure 14. Comparison of measured and calculated z-bending strain at RA763

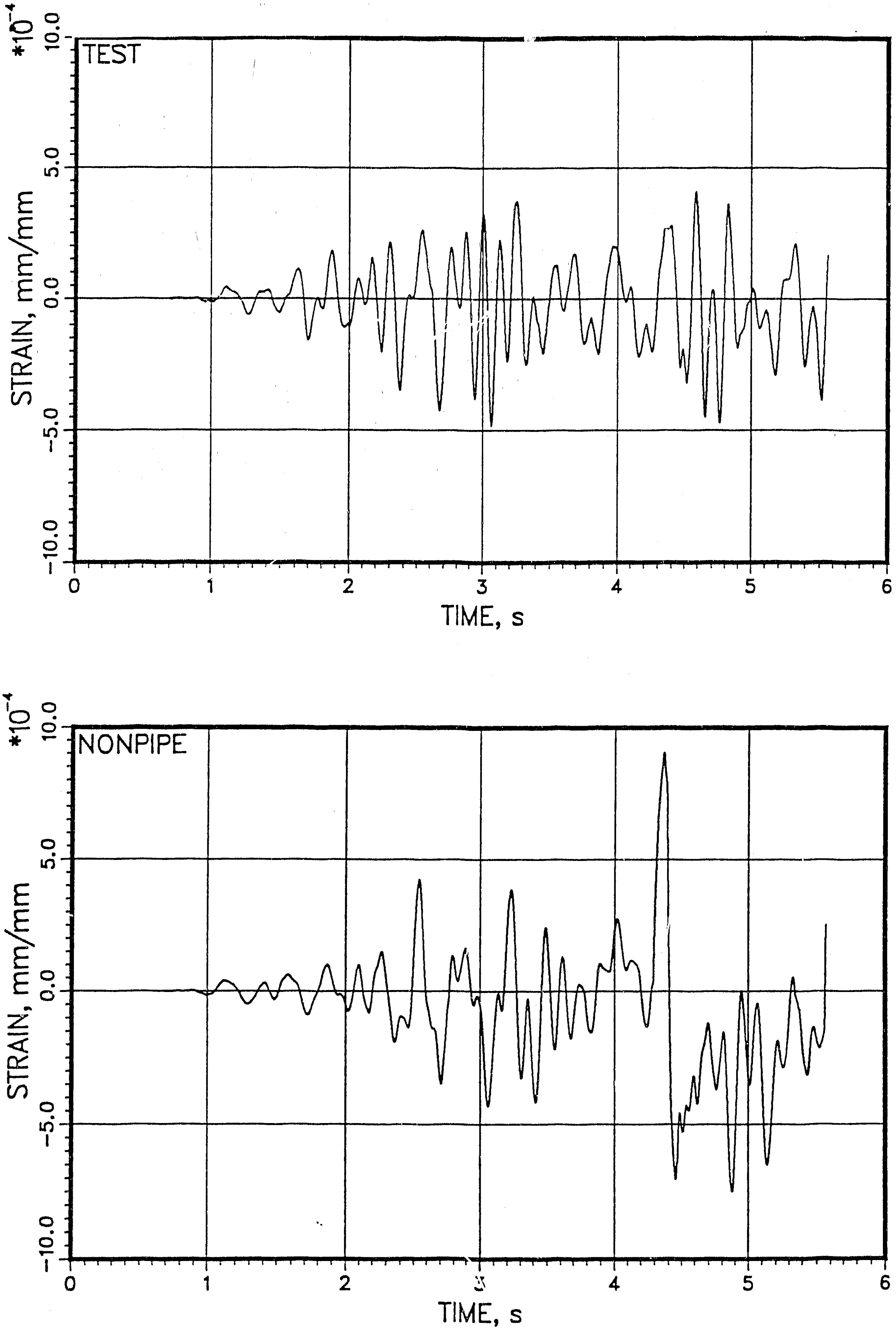

Figure 15. Comparison of measured and calculated shear strain at RA760

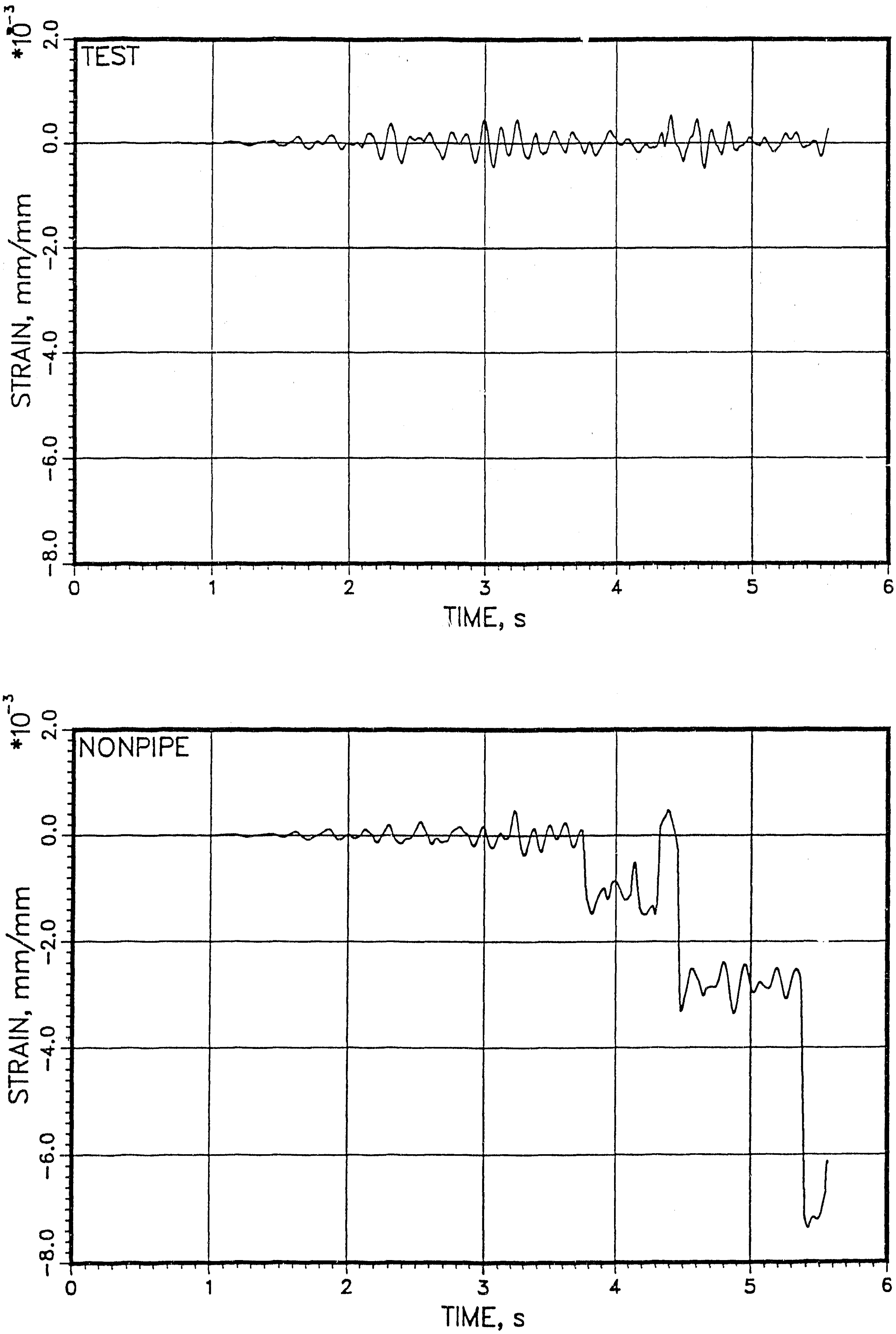

Figure 16. Comparison of measured and calculated shear strain at RA763

END

DATE FILMED

05 / 08 / 91